LETTERS
PUBLISHED ONLINE: 8 NOVEMBER 2009 | DOI: 10.1038/NGEO684
nature geoscience

Deep creep as a cause for the excess seismicity along the San Jacinto fault

Shimon Wdowinski*

Since 1890, the San Jacinto fault in Southern California has been the site of eleven earthquakes of moderate magnitude ($6 < M < 7$) and tens of thousands of small earthquakes, but none of large magnitude[1,2]. This activity contrasts sharply with the seismic quiescence of the nearby southern San Andreas fault. Although this fault slips at a rate higher than that associated with the San Jacinto fault—23–27 mm yr^{-1} versus 12–22 mm yr^{-1} (refs 3, 4)—it has produced very few earthquakes and no moderate or larger events in historical times. Here I use recent seismic and geodetic data to reveal that at depths of 10–17 km within the seismogenic (brittle) crust, the San Jacinto fault is creeping and releasing elastic strain by many small earthquakes. As a result, the accumulation of strain along this fault occurs mostly in its upper 10 km; moderate earthquakes are likely to be sufficient to release such strain. In contrast, the southern San Andreas fault accumulates elastic strain throughout its vertical extent in the seismogenic crust, which will most probably be released by stronger earthquakes.

Earthquakes are the most familiar and best studied mechanism of crustal elastic strain release, but not the only one. Other strain release mechanisms include postseismic after-slip, slow slip events and aseismic creep. These mechanisms indicate that a significant amount of elastic strain can be released steadily or episodically in between moderate or large earthquakes. Here I present another mechanism of elastic strain release, deep creep, occurring within the lower section of the seismogenic crust at depths of 10–17 km.

This study relies on quantitative estimates of elastic strain accumulation and release along the southern San Andreas fault (SSAF) and the San Jacinto fault (SJF) as derived from geodetic and seismic observations and summarized in Table 1. The distribution and rate of strain accumulation are estimated from geodetic observations of interseismic crustal movements combined with dislocation models (see the Methods section). Elastic strain release is best determined from seismic observations, whereas aseismic strain release can be determined indirectly using geodetic measurements.

Interseismic crustal movements in Southern California indicate a high rate of shear strain accumulation along the active fault segments of the San Andreas Fault system[5] (SAFS). South of the Big Bend, where the SAFS branches into three parallel segments, the SSAF, SJF and the Elsinore fault, high-velocity gradients occur only along the SSAF and the SJF (Fig. 1 and Supplementary Fig. S1). Using dislocation models, various studies estimated the strain accumulation rate along the SJF at 12–22 mm yr^{-1} and along the SSAF at 23–27 mm yr^{-1} (Table 1 and Supplementary Table S1). Another important parameter calculated by these models is the locking depth, which is found to be 11 ± 2 km for the SJF and is 16 ± 2 km for the SSAF.

Elastic strain release can be estimated from earthquake catalogues of recorded seismicity and historical documents. The most accurate seismic record at present is the catalogue of relocated earthquakes in Southern California, containing 430,000 events for the time period 1981–2005 (ref. 1). Further information on larger events can be obtained from historical catalogues[2]. However, the seismic record provides only partial information on elastic strain release. Our knowledge of slow aseismic release is rather limited, because surface geodetic measurements are not very sensitive to small movements in the deep subsurface. Nevertheless, a deep aseismic strain release event on the SJF has been recorded by strain meters[6].

The epicentral map of Southern California (Fig. 1) shows high seismic activity along the SJF. To detect spatiotemporal seismic patterns along the SJF, I explored the relationships between depth, time and distance along the fault of more than 44,000 events found in the seismic catalogue[1] within a 10-km-wide swath along the fault trace. Although geological studies indicate that the SJF consists of nine or more distinctive segments[7], I divided the 230-km-long fault into three segments (Fig. 1) on the basis of geometrical considerations and spatiotemporal seismic patterns.

The most interesting and indicative activity occurs along the 120-km-long central segment. The depth–distance relationships (Fig. 2b) show the following three important observations: (1) most (66%) of the earthquakes nucleate at depths of 10–17 km (Fig. 2h), (2) most of the stronger events ($M > 4$) and consequently seismic moment release (92%) also occur at depths of 10–17 km and (3) the depth of the seismogenic crust is not uniform along the fault; it has an overall northwestward tilt. This trend was noticed before and was attributed to higher heat flow near the southern portion of the fault[8]. The depth–time relationships of the central segment (Fig. 2e) also show a larger distribution of stronger events at depths of 10–17 km. However, more importantly, these relationships show steady (time-wise) activity along the fault, indicating a continuous release of seismic strain with time. Seismic activity along the northern segment of the SJF shows depth–distance (Fig. 2a) and depth–time (Fig. 2d) relationships that are similar to the central segment. The main difference is a change in the depth of the seismogenic crust near the intersection with the SAF.

Seismic activity along the southern segment is very different compared with the two other segments (Fig. 2c). Seismicity is dominated by the 1987, $M = 6.6$ Superstition Hill earthquake, which released most of the seismic strain within a short time period (Fig. 2f). The earthquake nucleated at a depth of 5.6 km and ruptured a 20-km-long and 10-km-deep fault plane. Most of the earthquakes in this segment occurred at depths of 5–8 km.

Further information on seismic strain release can be obtained from historical and early instrumental record catalogues. The recent catalogue of historic events[2] indicates high levels of activity along the SJF and almost no activity along the SSAF. Since 1890, the SJF has produced eleven moderate size earthquakes ($6 < M < 7$). Owing

Division of Marine Geology and Geophysics, University of Miami, 4600 Rickenbacker Causeway, Miami, Florida 33149-1098, USA.
*e-mail: shimonw@rsmas.miami.edu.

Table 1 | Geodetically, geologically and seismically determined rates of strain accumulation and release along the SSAF and SJF.

Observation	Parameter	SSAF	San Jacinto fault	Reference
	Length	250 km	230 km	
Accumulation (Geodesy)	Slip rate	25 ± 2 mm yr^{-1}	17 ± 5 mm yr^{-1}	3, 4
	Locking depth	16 ± 2 km	11 ± 2 km	3, 4
Release—long-term (Geology)		25 ± 5 mm yr^{-1}	12 ± 6 mm yr^{-1}	14, 15
Release—historical record (150 years)	Moderate-large earthquakes	0	11 moderate earthquakes ($6 < M < 7$)	2
	Total moment release (ΣM_0)	0	1×10^{27} dyn-cm	
	Release rate	0	13–14 mm yr^{-1}	
Release—seismic activity (1981–2006)	Number of earthquakes	7,328	44,044	1
	Average depth	10–15 km	10–17 km	
	Seismogenic depth	16 ± 2 km	17 ± 3 km	
	Total moment release (ΣM_0) (South of Anza)	3×10^{18} dyn-cm	2.4×10^{24} dyn-cm (1.4×10^{24} dyn-cm)	
	Release rate (South of Anza)	0	<1 mm yr^{-1} (3–4 mm yr^{-1})	

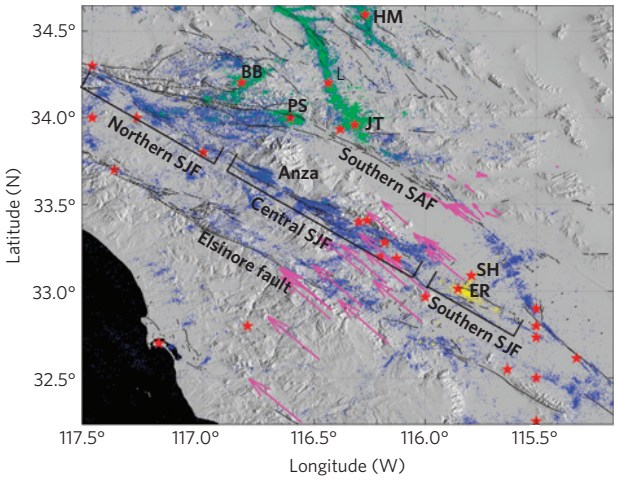

Figure 1 | Seismicity and crustal movements along the southern SAFS. The blue dots mark ongoing seismic events during the period 1981–2006 (ref. 1). The yellow dots mark three-month-long aftershock clusters following the 1987 Elmore Ranch (ER) and Superstition Hull (SH) earthquakes, and green dots mark aftershock dusters following the 1986 Palm Spring (PS), 1992 Joshua Tree (JT), 1992 Landers (L) and 1999 Hector Mine (HM) earthquakes. The red stars mark the location of moderate and strong events ($M > 6$) for the period 1800–2005 (ref. 2). The pink arrows mark a subset of geodetically observed crustal movements calculated with respect to stable North America[13]. The thin black lines mark the location of main fault segments and the thick lines mark the geographical locations of the three segments of the SJF shown in Fig. 2.

to the limited accuracy of the earlier record (before 1950), only four recent moderate events were located accurately enough. These four events nucleated at relatively shallow depths of 6–10 km, suggesting a high strain level in the shallow crust.

The seismic and geodetic observations provide two independent estimates concerning mechanical changes with depth. The seismically derived seismogenic depth describes the transition from brittle (earthquakes) to ductile deformation mechanisms. The geodetically derived locking depth describes the transition from continuous elastic deformation in the shallow subsurface to discontinuous motion (slip along dislocations) in the deeper section of the crust. It is often assumed that faults are locked throughout the entire seismogenic depth and slip occurs entirely in the ductile crust beneath. However, creeping or partially creeping fault segments in central and northern California indicate that significant slip can also occur within the seismogenic crust and is associated with seismic or micro-seismic activity.

A comparison between seismogenic and locking depths calculated for the SSAF and SJF (Table 1) shows significant mechanical differences between the two fault systems. For the SSAF, both the seismogenic and locking depth are similar (16 ± 2 km), indicating that the fault is locked throughout its entire seismogenic depth, which agrees well with the null seismicity along the SSAF. However, the seismogenic and locking depths calculated for the SJF, 17 ± 3 and 11 ± 2 km, respectively, are significantly different from each another, suggesting that a 'classic' locked-fault model is not valid here. The shallow locking depth indicates that steady motion along the fault also occurs within the seismogenic crust, in the depth range of 11–17 km, agreeing very well with the high level of seismic activity and seismic moment release at the same depth (Fig. 2).

On the basis of the above seismic and geodetic observations, I suggest that the SJF is subject to 'deep creep', a process that releases elastic strain both seismically and aseismically at the lower level of the seismogenic crust, at depths of 10–17 km. The deep creep can be viewed as the uppermost section of a dislocation extending upward from the ductile crust into the seismogenic crust (Fig. 3). It can also be viewed as a transition zone, a partially locked fault interface located between a fully locked segment above (upper 10 km) and a continuously slipping segment below. Similar transition zones have been found in subduction zones, where elastic strain is released aseismically by slow slip events followed by a large number of seismic tremors. Slow slip events in subduction zones occur at intermediate depths of 20–60 km, below the fully locked subduction interface but above the steady slip at depth[9].

Unlike slip in the ductile crust, which is assumed to occur continuously over time, deep creep in the seismogenic crust has an episodic component; at least the seismic strain is released in a discontinuous manner. The frequent occurrence of earthquakes, an average of four earthquakes per day ($M > 1.5$), generates a sense of a continuous process. However, the more indicative seismic

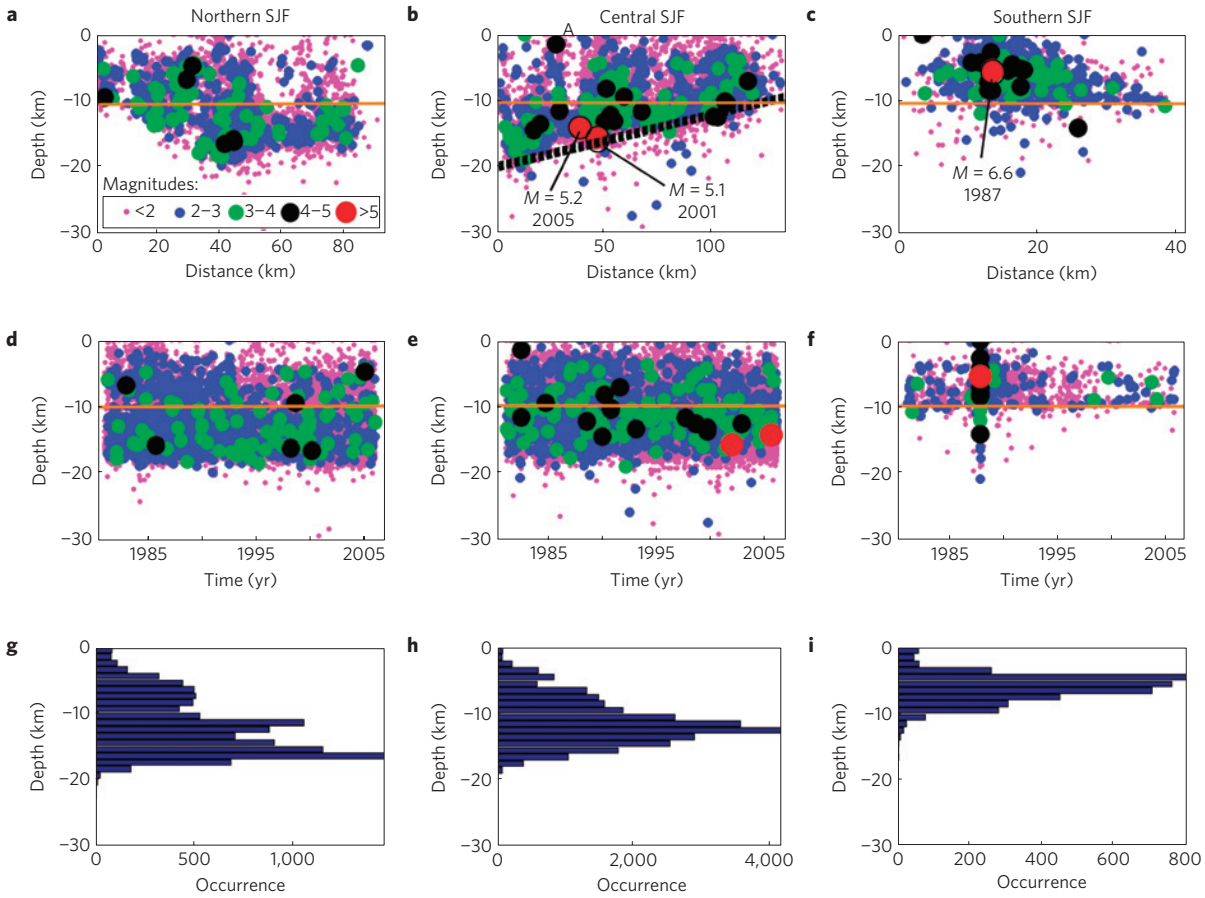

Figure 2 | Seismic activity along the San Jacinto fault. a, Hypocentre location along the northern segment. The orange line marks the geodetically determined locking depth. **b**, Hypocentres along the central segment. The dotted line marks the base of the seismogenic crust. 'A': Anza Gap. **c**, Hypocentres along the southern segment. **d**–**f**, Seismic activity as function of time showing that seismicity occurs regularly along the northern and central segments. The seismicity along the southern segment had a spike in activity following the 1987 Superstition Hill earthquake. **g**–**i**, Earthquake distribution with depth showing peak activity above the base of the seismogenic layer.

moment release, which is dominated by the higher magnitude events, suggests that elastic strain is released episodically.

The recent four moderate earthquakes ($6 < M < 7$) recorded along the SJF nucleated at shallow depths (6–10 km) and obviously are not part of the deep creep. These larger magnitude events are typical 'coseismic' earthquakes that rupture the locked section of the fault. As the SJF is locked only to 11 ± 2 km depth, the accumulated strain along the fault is relatively small and not sufficient to produce large events ($M > 7$).

Supporting evidence for the deep creep process can be obtained from the aftershock distribution of the two largest deep events ($M > 5$) that occurred in 2001 and 2005 south of the Anza Gap in the central segment. These two events nucleated at depths of 14–15 km and triggered hundreds of aftershocks. The aftershock distribution of each of the two events shows very clearly that the ruptured fault planes were long, narrow and located within the lower section of the seismogenic crust (Supplementary Fig. S2). Furthermore, the aseismic event following the 2005 earthquake was estimated to have a deep origin[6].

The total creep rate, as estimated from geodetic observations for SJF, is 12–22 mm yr^{-1} and contains both seismic and aseismic components. The seismic creep rate can be estimated from the summed seismic moment release and assumptions on the area of the creeping segments (see the Methods section). The estimated rate for the entire central segment (120 km long) creeping uniformly along the deepest 6 km of the seismogenic crust is less than 0.5 mm yr^{-1}, suggesting that most of the creep occurs aseismically.

The very different seismic levels occurring along the SSAF and the SJF reflect mechanical differences between the two fault systems. The commonly accepted explanation suggests that seismic productivity is controlled by the structural complexity of fault systems, in which strike-slip faults with a large cumulative geological offset have a smoother stress field along the fault and consequently produce less seismicity[10]. According to this explanation, the young and structurally complex SJF is seismically very productive, whereas the mature SSAF has a smooth fault structure and, hence, has a low seismic productivity. A different explanation based on a damage rheology model suggests that the earthquake productivity is controlled primarily by the heat flow and other factors that govern the effective viscosity of a given fault zone[11].

Here I propose an alternative explanation for the different activity level between the faults, a deep creep mechanism, which is based on the vertical distribution of earthquakes, as well as on the inferred locking depth derived from geodetic observations. The proposed mechanism explains well the high level of 'interseismic' seismicity along the SJF and the lack of seismicity along the SSAF. However, it does not explain the cause for the different mechanical behaviour. Possible explanations for this behaviour are a low frictional strength of the deeper section of the SJF and/or a high pore pressure, which effectively reduce the normal stresses along the fault and act as a weakening mechanism.

The different interseismic deformation occurring along the SSAF and SJF implies different hazards from the two fault systems.

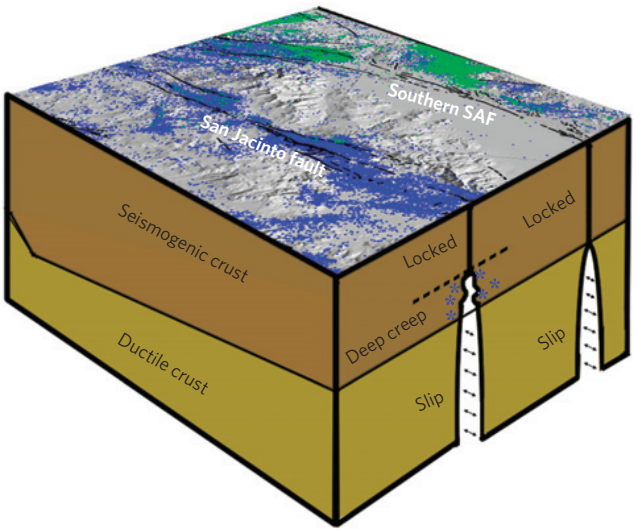

Figure 3 | Interseismic strain accumulation and release mechanisms along the southern SAFS. Both the SSAF and SJF accumulate elastic strain owing to steady slip in the ductile crust, beneath the faults. The SSAF is locked throughout the seismogenic crust and does not generate interseismic earthquakes. The SJF is locked only in the upper 10 km and creeps seismically and aseismically above the base of the seismogenic crust, which is tilted northwestward, at depths of 10–17 km. The blue asterisks represent schematic hypocentre locations. The blue and green dots on the shaded relief plot mark ongoing seismicity and aftershock clusters, respectively.

The SJF accumulates elastic strain only in its upper 10 km and, hence, can release only a limited amount of seismic energy, which explains the moderate magnitude of the eleven historical coseismic events. The SSAF, which is locked throughout its entire seismogenic depth (0–16 km), accumulates significantly more elastic strain. Consequently, when ruptured, the SSAF will release more energy by stronger earthquakes.

Methods

Geodetic slip rate estimates. Geodetic measurements conducted in seismically active areas reveal that during the interseismic stage of the earthquake cycle, elastic strain accumulates along active fault segments. These observations are best explained by dislocation models assuming that faults are locked at the upper section of the crust, typically throughout the seismogenic crust and that the crust deforms elastically owing to continuous slip along a dislocation surface located from the base of the locked fault downward. Simple dislocation models of infinitely long fault segments depend on two parameters, slip rate and locking depth, which are constrained by geodetic observations. More evolved models may account for complex fault geometry, inhomogeneous slip distribution on the dislocation surface and non-elastic rheology.

The range in the slip rate and locking depth estimates (Table 1) reflects a contribution of two sources. One is derived from uncertainties in fitting a dislocation model to a geodetic data set. The other reflects differences among studies that use different model assumptions and observations (Supplementary Table S1). In this study, I use the locking depth calculated by two recent studies[3,4]. Earlier studies that used limited data sets yielded a shallower locking depth (5–10 km). A detailed list of slip rate and locking depth estimates is provided in Supplementary Table S1.

Seismic slip rate estimates. The average seismic slip rate can be estimated from the summed contribution of the seismic moment released along a fault over a finite time period. It is given by

$$\bar{u} = \frac{1}{\mu A \Delta T} \sum_{\Delta T} M_0 \qquad (1)$$

where A is the fault area, μ is the shear modulus (assumed to be 30 GPa), ΔT is the data time span and M_0 is the seismic moment[12]. M_0 is scaled to the magnitude (M) using the following formula: $M_0 = 10 \times \exp\{1.5 \times M + 16.1\}$.

Using the above equation, I calculated the seismic creep rate for the central segment of the SJF, which is the most active seismic segment. I assumed that the 120-km-long fault segment creeps along the bottom 6 km of the seismogenic crust (depths of 11–17 km) and calculated a very low seismic creep rate of less than 0.5 mm yr^{-1}. However, the strain release is unevenly distributed in both space and time. By considering the more seismically active area located south of the Anza Gap, where the two larger events (M > 5) occurred (Supplementary Fig. S2), I calculated a creep rate of 3 mm yr^{-1} for the entire 25 yr duration of the catalogue.

The summed moment estimates should be used very carefully, because they are biased owing to the finite length of the available seismic catalogues. However, it is still important to calculate the seismic creep rate as it shows that the seismic rate is very small compared with the total (geodetic) creep rate. Despite the limited record, the calculated creep rate is still valuable, because moderate and large earthquakes along the SJF are coseismic events. Thus, they are not considered in the seismic creep rate calculations and do not affect the estimated rate. The seismic catalogue used in this study contains two M > 5 events, which are probably the largest magnitude earthquakes to occur in the deep creep zone. The contribution of these events to the calculated creep rate is still fairly minor, because the total seismic creep rate for the entire length of the fault is only 0.5 mm yr^{-1}. Thus, more M < 5.5 earthquakes will not have a significant influence on the calculations.

Received 3 February 2009; accepted 6 October 2009; published online 8 November 2009

References

1. Lin, G. Q., Shearer, P. M. & Hauksson, E. Applying a three-dimensional velocity model, waveform cross correlation, and cluster analysis to locate southern California seismicity from 1981 to 2005. *J. Geophys. Res.* **112,** B12309 (2007).
2. Kagan, Y. Y., Jackson, D. D. & Rong, Y. A new catalog of southern California earthquakes, 1800–2005. *Seismol. Res. Lett.* **77,** 30–38 (2006).
3. Fialko, Y. Interseismic strain accumulation and the earthquake potential on the southern San Andreas fault system. *Nature* **441,** 968–971 (2006).
4. Wdowinski, S., Smith-Konter, B., Bock, Y. & Sandwell, D. Diffuse interseismic deformation across the Pacific–North America plate boundary. *Geology* **35,** 311–314 (2007).
5. Wdowinski, S., Sudman, Y. & Bock, Y. Geodetic detection of active faults in S. California. *Geophys. Res. Lett.* **28,** 2321–2324 (2001).
6. Agnew, D. & Wyatt, F. *SCEC Annual meeting* (SCEC, 2005).
7. Sanders, C. & Magistrale, H. Segmentation of the northern San Jacinto fault zone, southern California. *J. Geophys. Res. B* **102,** 27453–27467 (1997).
8. Doser, D. I. & Kanamori, H. Depth of seismicity in the Imperial Valley region, (1977–1983) and its relationship to heat flow, crustal structure, and the October 15, 1979, earthquake. *J. Geophys. Res.* **91,** 675–688 (1986).
9. Schwartz, S. Y. & Rokosky, J. M. Slow slip events and seismic tremor at circum-pacific subduction zones. *Rev. Geophys.* **45,** RG3004 (2007).
10. Wesnousky, S. G. Seismicity as a function of cumulative geologic offset—some observations from Southern California. *Bull. Seismol. Soc. Am.* **80,** 1374–1381 (1990).
11. Ben-Zion, Y. & Lyakhovsky, V. Analysis of aftershocks in a lithospheric model with seismogenic zone governed by damage rheology. *Geophys. J. Int.* **165,** 197–210 (2006).
12. Brune, J. N. Seismic moment, seismicity and rate of slip along major fault zones. *J. Geophys. Res.* **73,** 777–784 (1968).
13. Shen, Z.-K. *et al.* The SCEC Crustal Motion Map, Version 3.0. (2003).
14. Working Group on California Earthquake Probabilities. Seismic hazard in Southern California: Probable earthquakes, 1994 to 2024. *Bull. Seismol. Soc. Am.* **85,** 379–439 (1995).
15. Working Group on California Earthquake Probabilities. The Uniform California Earthquake Rupture Forecast, Version 2 (UCERF 2). *USGS Open File Report 2007-1437* (USGS, 2007).

Acknowledgements

I thank Y. Ben-Zion, T. Dixon, F. Amelung and S. Eriksson for their comments and suggestions. I am also grateful to D. Jackson for his very helpful review. The relocated earthquake catalogue was provided by G. Lin.

Additional information

Supplementary information accompanies this paper on www.nature.com/naturegeoscience. Reprints and permissions information is available online at http://npg.nature.com/reprintsandpermissions.